Direct Interaction of Multidrug Efflux Transporter AcrB and Outer Membrane Channel TolC Detected via Site-Directed Disulfide Cross-Linking†

Norihisa Tamura,[‡,§] Satoshi Murakami,[‡,§,||] Yoshiaki Oyama,[⊥] Masaji Ishiguro,[#] and Akihito Yamaguchi*[,‡,§]

Department of Cell Membrane Biology, Institute of Scientific and Industrial Research, Osaka University, Ibaraki, Osaka 567-0047, Japan, Graduate School of Pharmaceutical Sciences, Osaka University, Suita, Osaka 565-0871, Japan, CREST, Japan Science and Technology Agency, Osaka, Japan, PRESTO, Japan Science and Technology Agency, Osaka, Japan, Daiichi Suntory Biomedical Research Company, Ltd., Shimamoto, Osaka 618-8513, Japan, and Suntory Institute for Bioorganic Research, Shimamoto, Osaka 618-8503, Japan

Received March 11, 2005; Revised Manuscript Received June 10, 2005

ABSTRACT: The AcrAB−TolC system exports a wide variety of drugs and toxic compounds, and confers intrinsic drug tolerance on *Escherichia coli*. The crystal structures suggested that AcrB and TolC directly dock with each other. However, biochemical and biophysical evidence of their interaction has been contradictory until recently. In this study, we examine the interaction sites by means of in vivo disulfide cross-linking between cysteine residues introduced by site-directed mutagenesis at the tops of the vertical hairpins of AcrB and the bottoms of the coiled coils of polyhistidine-tagged TolC molecules, which are structurally predicted docking sites. The AcrB−TolC complex formed through disulfide cross-linking was detected when a specific pair of mutants was coexpressed in *E. coli*. Our observations suggested that the AcrB−TolC complex may be formed through a two-step mechanism via transient tip-to-tip interaction of AcrB and TolC. The cross-linking was not affected by AcrA, the substrate, or a putative proton coupling site mutation.

The AcrAB−TolC system is a multicomponent transporter and is responsible for the intrinsic drug tolerance of *Escherichia coli* (*1*, *2*). AcrAB−TolC, coupled with a proton motive force, pumps out a wide variety of antibiotics, dyes, and detergents not only from the cytoplasm but also from the periplasm through the TolC duct (*3*). Therefore, AcrAB−TolC confers resistance to β-lactams (*4*), which inhibit the enzymes on the periplasmic surface of the plasma membrane. AcrA is a membrane fusion protein (*5*), AcrB an inner membrane protein (*6*), and TolC an outer membrane protein (*7*). AcrAB requires TolC to confer drug resistance (*8*), so AcrA, AcrB, and TolC are thought to form a complex.

TolC is composed of a homotrimer having a uniform channel and has a 10 nm long α-helical domain that projects across the periplasmic space (*9*). Because the periplasmic entrance of TolC is blocked by twisted inner and outer coiled coils, opening of the periplasmic entrance is necessary for protein export (*10*).

AcrB also comprises a trimer, and consists of a large periplasmic domain and a transmembrane region of approximately 7 and 5 nm, respectively (*3*). The total periplasmic length of AcrB and TolC is 17 nm, which is close to the shortest periplasmic width (*11*) and is enough to span the periplasm, so AcrB is thought to be able to interact directly with TolC. There are open vestibules between the AcrB protomers on the periplasmic surface of the plasma membrane. Each vestibule is postulated to be an entrance for substrates and is connected via the central pore to the funnel at the top of AcrB (*12*). The TolC docking domain at the top of AcrB fits with that of TolC when the AcrB trimer is docked with the TolC trimer (*3*). These data strongly imply a direct interaction between AcrB and TolC (Figure 1).

Recently, the crystal structure of MexA, which is a homologue of AcrA, was determined at 2.4 (*13*) and 3.0 Å (*14*). AcrA was modeled as a ring surrounding AcrB and TolC. Therefore, AcrB is more likely to interact directly with TolC, but the complex between the two proteins was not confirmed until recently.

The interaction between AcrA and AcrB was detected on chemical cross-linking (*15*) and copurification (*16*). However, it was difficult to detect the intermembrane AcrAB−TolC complex. Recently, Tikhonova and Zgurskaya detected the AcrAB−TolC complex in the presence of AcrA on cofractionation and chemical cross-linking (*17*). This observation does not exclude the possibility that AcrA acts as an adaptor for the AcrB−TolC interaction. Touzé et al. first detected the AcrB−TolC complex in the absence of AcrA on in vivo chemical cross-linking with a 12 Å spacer of dithiobissuccinimidylpropionate (DSP) (*18*). Their results indicate the proximity of AcrB and TolC. However, since AcrB did not experience a change in enthalpy when TolC was added, they thought that no stable interaction was possible without AcrA (*18*).

† This work was supported by Grants-in-Aid from the Ministry of Education, Culture, Sports, Science and Technology of Japan.

* To whom correspondence should be addressed. E-mail: akihito@sanken.osaka-u.ac.jp. Phone: +81-6-6879-8545. Fax: +81-6-6879-8549.

‡ Osaka University.

§ CREST, Japan Science and Technology Agency.

|| PRESTO, Japan Science and Technology Agency.

⊥ Daiichi Suntory Biomedical Research Co., Ltd.

Suntory Institute for Bioorganic Research.

10.1021/bi050452u CCC: $30.25 © 2005 American Chemical Society
Published on Web 07/29/2005

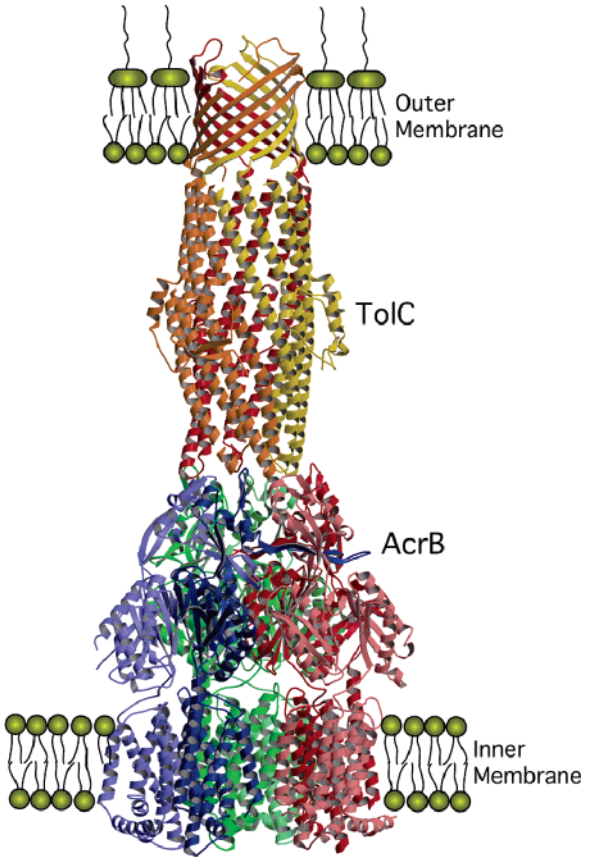

FIGURE 1: Proposed model of the AcrB−TolC complex. The 3-fold axes of AcrB and TolC were aligned, to maximize the surface complementarity (*33*) and the buried surface area (*34*). This figure was generated with MOLSCRIPT (*35*) and Raster3D (*36*).

In this study, we introduced Cys residues into AcrB and TolC by site-directed mutagenesis, and then the AcrB−TolC complex was detected on spontaneous disulfide cross-linking in vivo. This method makes it possible to determine the interaction sites precisely. To investigate the formation of the AcrAB−TolC complex and the mechanism for the export of substrates, it is important to identify the interaction sites.

EXPERIMENTAL PROCEDURES

Bacterial Strains and Plasmids. E. coli strains JM109 (*19*), CJ236 (*20*), and W3104 (*21*) were used for DNA manipulation, site-directed mutagenesis by the Kunkel method, and investigation of the phenotypes of the mutants, respectively. Strain W3104ΔacrAB (*22*) is an *acrAB* gene-deletion derivative of *E. coli* W3104. Plasmid pACBHLR, a derivative of pUC118 that carries the *acrR*, *acrA*, and His-tagged Cys-less *acrB* genes, was described previously (*3*). Plasmid pACBLR2, a derivative of pACBHLR, has an ApaI site at the end of the *acrA* gene and no His tag at the end of the *acrB* gene. Plasmid pACRBLR, a derivative of pACBLR2, lacks the *acrA* gene. Plasmid pKO3 was a gift from G. M. Church (*23*). Plasmid pKO3 is a gene replacement vector that contains a temperature-sensitive origin of replication, and markers for positive and negative selection for chromosomal integration and excision.

Cloning of the tolC Gene and Construction of Plasmids. The full-length *tolC* gene was cloned from the *E. coli* W3104 chromosome by means of the PCR[1] method using synthetic oligonucleotides 5′-gaggatccgatgacgaaatctataaagatc-3′ and 5′-tgcagcatgctaatgatgatgatgatggttacggaaagggttatgaccgtt-3′ as forward and reverse primers, respectively. The resulting fragment was digested with BamHI and SphI restriction enzymes, followed by insertion into pACYC184 at the BamHI−SphI site. The resulting plasmid, named pACYC-tolCH, carries the 318 bp upstream region containing the native promoter and a 3′-His tag, in addition to the *tolC* gene.

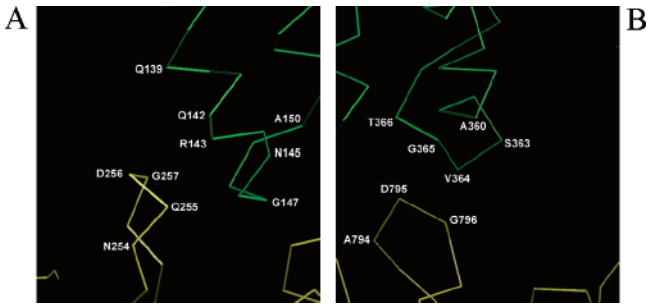

FIGURE 2: Close-up views of the docking sites of the AcrB−TolC complex model. α-Carbon tracings of AcrB and TolC are shown in yellow and green, respectively. Mutated residues are colored white: (A) the N-terminal region of the site and (B) the C-terminal region of the site.

Gene Disruption. The chromosomal *tolC* gene was deleted by means of in-frame crossover polymerase chain reaction, and then the deletion was introduced into the *E. coli* W3104ΔacrAB (*22*) chromosome by means of plasmid pKO3 (*23*). The resulting strain was named *E. coli* W3104ΔacrABΔtolC. The gene deletion was confirmed by the length of the PCR fragment of the chromosomal *tolC* gene.

In Vivo Spontaneous Disulfide Cross-Linking Assay. Strains carrying pairs of plasmids were grown in medium A supplemented with 0.1% casamino acids and 0.2% glucose. Cultures were incubated at 30 °C, with aeration, and harvested by centrifugation when the OD_{530} reached 0.9. Cells were disrupted by brief sonication with *N*-ethylmaleimide. Membrane fractions were collected by ultracentrifugation. The resulting samples were boiled for 3 min in nonreducing sample buffer containing 4 M urea before analysis by SDS−PAGE and Western blot analysis.

Purification of the AcrB−TolC Complex. Cells were cultivated in medium A supplemented with 0.1% casamino acid and 0.2% glucose at 37 °C. Harvested cells were disrupted with a Microfluidizer M-110EH (Microfluidics Corp.), and the membrane fraction was collected and washed via several ultracentrifugation steps at 150000*g* for 90 min. The purified membranes were resuspended in buffered glycerol [50 mM Tris-HCl (pH 7.0) and 10% glycerol]. Then the membrane proteins were solubilized in 2% *n*-dodecyl *β*-D-maltoside (DDM) (Glycon Biochemicals GmbH). Lipids and debris were removed by ultracentrifugation at 170000*g* for 60 min. The extracted molecular complex of histidine-tagged AcrB and TolC was purified by affinity column chromatography on Chelating Sepharose Fast Flow (Amersham Bioscience Corp.) immobilized with Ni^{2+} equilibrated with buffer [20 mM Tris-HCl (pH 7.5), 0.3 M NaCl, 10% glycerol, and 0.2% DDM]. The column was washed with 25 mM imidazole in the buffer described above. The

[1] Abbreviations: PCR, polymerase chain reaction; SDS−PAGE, sodium dodecyl sulfate−polyacrylamide gel electrophoresis; Ni−NTA, Ni−nitrilotriacetic acid.

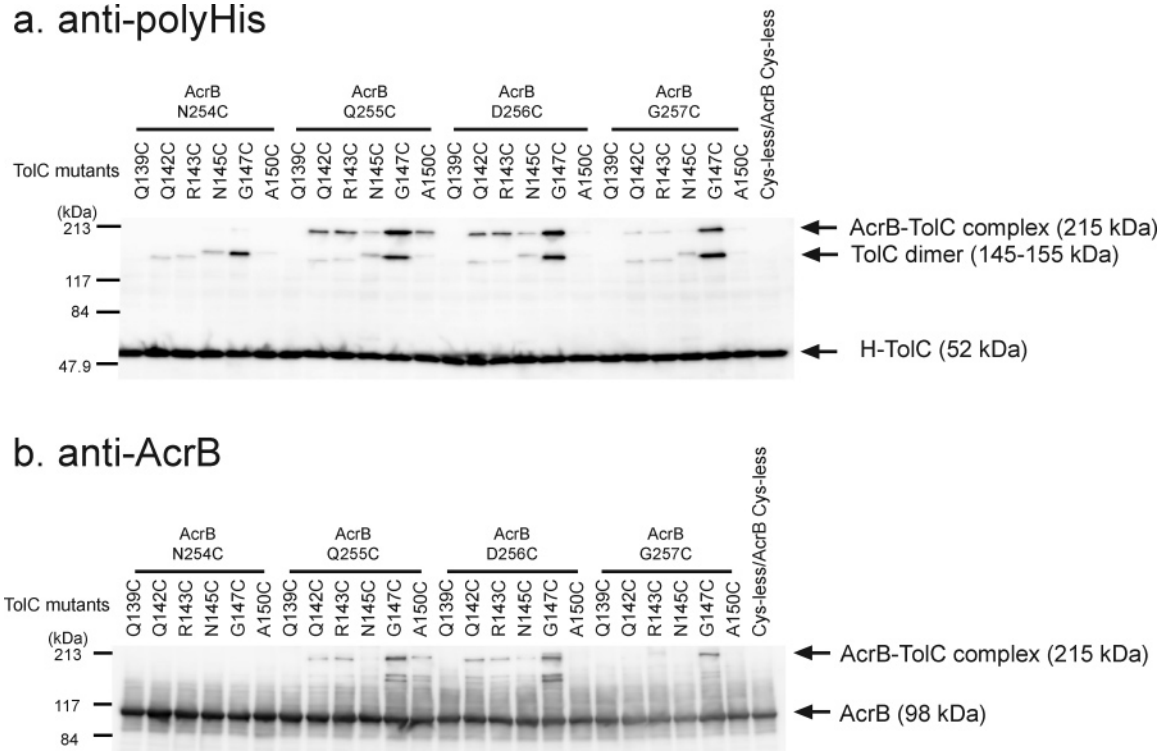

FIGURE 3: Site-specific in vivo spontaneous disulfide cross-linking between CL-AcrB and H-TolC in the N-terminal region Cys mutants. Membrane fractions were obtained from the strains expressing the indicated combinations of Cys mutants of CL-AcrB and H-TolC as described in Experimental Procedures, followed by separation by SDS−PAGE under nonreducing conditions. AcrB and H-TolC were detected via immunoblot analysis using anti-polyhistidine (A) and anti-AcrB (B) antibodies, respectively.

imidazole concentration was increased gradually to elute the AcrB−TolC complex.

SDS−PAGE and Western Blot Analysis. The membrane proteins were resolved by SDS−PAGE with 7.5% acrylamide using the discontinuous buffer system of Laemmli (*24*). The resolved proteins were transferred from the gels to polyvinylidene difluoride membranes by transverse electrophoresis. AcrB and TolC proteins were detected by Western blotting with an anti-AcrB rabbit antibody (*12*) and an anti-polyHis mouse antibody (Sigma), respectively.

RESULTS

Formation of Disulfide Linkages between Cys-Introduced AcrB and TolC. First, two intrinsic Cys residues (Cys493 and Cys887) of AcrB were replaced with Ala by site-directed mutagenesis to construct Cys-less AcrB (CL-AcrB). TolC has no intrinsic Cys residues. Then, we introduced a single cysteine residue into CL-AcrB and TolC at the postulated AcrB−TolC contact positions by site-directed mutagenesis. The mutated Cys residues are represented with white characters in Figure 2.

Paired combinations of plasmid pACBLR2 expressing AcrA and CL-AcrB Cys variants and plasmid pACYCtolCH expressing polyhistidine-tagged TolC (H-TolC) Cys variants were introduced into strain W3104ΔacrABΔtolC, which is a multidrug hypersensitive strain. All pairs of mutants gave a multidrug resistance phenotype (data not shown), indicating that the cysteine mutations did not affect the activity. W3104ΔacrABΔtolC cells expressing AcrA, the CL-AcrB Cys mutant, and the H-TolC Cys mutant at the mid-log phase of growth were sonicated in the presence of *N*-ethylmaleimide (NEM) to prevent further disulfide bond formation. Membrane proteins collected via ultracentrifugation were analyzed by SDS−PAGE and immunoblotting under nonreducing conditions.

Figure 3 shows the results of immunoblot analysis of the mutants with respect to the N-terminal regions of CL-AcrB and H-TolC. In addition to the TolC monomer (52 kDa), dense bands of cross-linked products of 215 and 155 kDa were detected with anti-poly-His antibodies with the combinations of the Q255C, D256C, and G257C mutants of CL-AcrB with the G147C mutant of H-TolC (Figure 3A). Significant cross-linked products of 215 kDa were also detected with the combinations of the Q255C and D256C mutants of CL-AcrB with the Q142C and R143C mutants of H-TolC, and the combination of Q255C CL-AcrB with A150C H-TolC. The 215 kDa cross-linked products were also detected with anti-AcrB antibodies with the same combinations of Cys mutants of CL-AcrB and H-TolC (Figure 3B), indicating that they represent the AcrB−TolC complex. In addition, two closely contiguous bands were also detected around 160 kDa with anti-AcrB antibodies with the combinations of Q255C and D256C CL-AcrB with G147C H-TolC.

To identify the components of these cross-linked products, proteins from strains expressing D256C CL-AcrB and G147C H-TolC were purified by Ni−NTA chromatography, and then the purified proteins were analyzed by SDS−PAGE and immunoblotting (Figure 4). The purified proteins gave four bands (52, 98, 155, and 215 kDa) on Coomassie brilliant blue staining (Figure 4A). In the presence of reducing agent 2-mercaptoethanol (2-ME), the 215 and 155 kDa bands disappeared, splitting into 98 and 52 kDa bands, respectively, confirming these bands represent cross-linked products. The

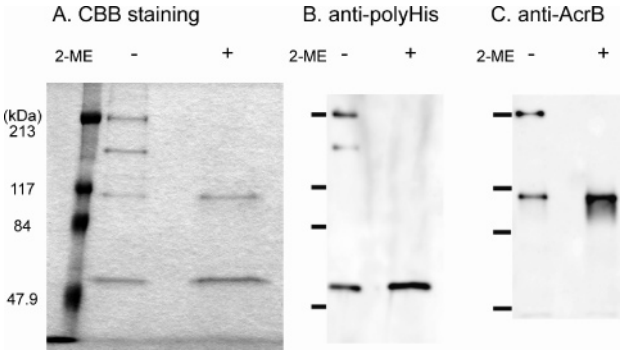

FIGURE 4: Purification and immunoblot analysis of the cross-linked complex of the D256C mutant of CL-AcrB and the G147C mutant of H-TolC. The complex was purified by Ni^{2+}-chelate column chromatography, and then separated by SDS−PAGE in the absence or presence of 2-mercaptoethanol (2-ME). AcrB and H-TolC were analyzed by Coomassie brilliant blue staining (A) and immunoblotting using anti-polyhistidine (B) and anti-AcrB (C) antibodies, respectively.

anti-poly-His antibodies visualized the 215, 155, and 52 kDa bands (Figure 4B), while the anti-AcrB ones visualized the 215 and 98 kDa bands (Figure 4C). Therefore, it is clear that the 215, 155, 98, and 52 kDa bands correspond to the AcrB−TolC complex, the TolC homodimer, the AcrB monomer, and the TolC monomer, respectively. There was no band around 160 kDa with the anti-AcrB antibodies. Therefore, the bands around 160 kDa observed in Figure 3B might be partially degraded AcrB dimers. Since the calculated molecular masses of AcrB and TolC are 114 and 51 kDa, respectively, the electrophoretic mobilities of the AcrB−TolC complex and TolC dimer are significantly different from those estimated from their molecular masses, probably due to the elongated form of the cross-linked products. The reason the purified proteins contained a small amount of AcrB monomer even under nonreducing conditions might be that AcrB is slightly copurified on a Ni−NTA column because of the presence of two histidine residues at the C-terminal end of AcrB.

Figure 5 shows the formation of a cross-linked complex in the case of the C-terminal region. In addition to the 52 kDa TolC monomer band, 195 and 140 kDa bands were detected with anti-poly-His antibodies with the combinations of the D795C and G796C mutants of CL-AcrB with the G365C mutant of H-TolC (Figure 5A). The 140 kDa band was also observed for the T366C mutant of H-TolC. Since the 195 kDa band was also detected with the anti-AcrB antibodies but the 140 kDa band was not detected with these antibodies (Figure 5B), the 195 and 140 kDa bands correspond to the AcrB−TolC complex and the TolC dimer, respectively. The difference in apparent molecular mass between the cross-linked products of the C-terminal and N-terminal regions might be due to the slight difference in the complex structure.

Effects of AcrA, Acriflavine, and a Proton Motive Force on the Formation of AcrAB−TolC Complexes. To determine what is needed for formation of the AcrB−TolC complex, attempts were made to detect the cross-linked products under various conditions: in the absence of AcrA, in the presence of acriflavine (a good substrate for AcrB) in the culture medium, and with the D407A mutation of AcrB. Asp407 is judged to be essential for proton translocation (3). The D256C mutant of CL-AcrB and the G147C mutant of H-TolC were used in this experiment. When AcrB was expressed from plasmid pACRBLR, which only carries the *acrR* and *acrB* genes, i.e., not the *acrA* gene, the amount of cross-linked product was almost the same as in the presence of AcrA (data not shown). Acriflavine and the mutation at Asp407 also did not affect cross-link formation (data not shown). Therefore, neither AcrAB complex formation, substrate binding, nor protonation of AcrB appears to affect formation of the AcrB−TolC complex.

DISCUSSION

We have detected the direct interaction between the top of AcrB and the bottom of TolC using site-directed in vivo disulfide cross-linking without the use of a cross-linking reagent. The formation of spontaneous disulfide bonds suggests that the Cys residue of AcrB is very close to that of TolC in the AcrAB−TolC ternary complex, confirming our direct docking model (*3*). Disulfide bond formation is highly dependent on the position of cysteine insertion. The cross-linkable positions are all located around the tips of the vertical hairpins in AcrB and the coiled coils of TolC (Figure 2A). Therefore, there is no doubt about that the AcrB−TolC interaction comprises a head-to-tail interaction in these regions. However, it should be noted that the only hitherto-obtained structures of AcrB and TolC are those in their separate states. Until contact, they are expected to be in the closed form (*3*, *9*). Their conformations, especially around the contact sites, should greatly change when they are docked. Thus, the close-up views of the docking sites shown in Figure 2 do not correctly reflect the actual structures of the docking sites when they are docked. When we observe the close-up views considering this restriction, we find that points in most contact, positions 255, 256, and 257, in AcrB are all at the tip of the vertical hairpin on the N-terminal side. In addition, the counterpart, position 147, in TolC is also located at the tip of the coiled coil on the N-terminal side of TolC. However, the sites in second-most contact, positions 142, 143, and 150, in TolC are several residues apart from the tip of TolC. Although all of these residues could be put at positions that can interact with the tip of the AcrB hairpin in the modified conformation, it would be an unnatural forced structure. The preferable interpretation is a two-step contact mechanism (Figure 6), that is, a first tip-to-tip interaction followed by a change to a deeply cogwheel-like meshed interaction. The disulfide bonds between Q255C, D256C, and G257C of AcrB and G147C of TolC might be fixed at the first tip-to-tip contact stage. At the second meshed stage, a conformational change of AcrB and TolC might occur that brings the residue at position 150 of TolC close to positions 255 and 256 of AcrB, like the proximity between positions 142 and 143 of TolC and positions 255 and 256 of AcrB, probably with a slight twist of the coiled coils. In addition, position 257 of AcrB may also be a little separated from the contact site in the meshed structure. The reason the degree of cross-linking at the second stage is lower than that at the first stage might be that most of them are separated after a short tip-to-tip contact, and only a few of them are involved in the formation of the stable complex.

In the C-terminal half, the conformational change is expected to be greater than that in the N-terminal half, because the closed conformation of TolC may be due to the twisted-up structure of the coiled coils on the C-terminal side

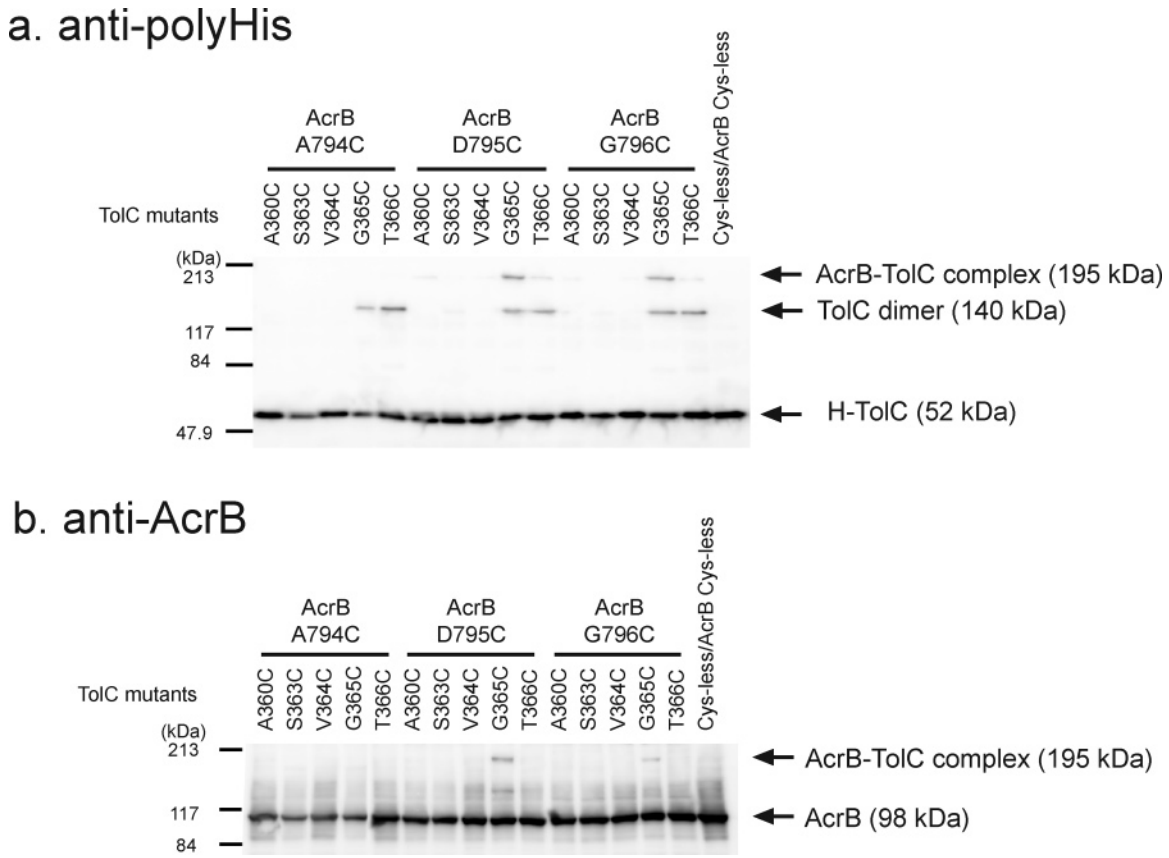

FIGURE 5: Site-specific in vivo spontaneous disulfide cross-linking between CL-AcrB and H-TolC in the C-terminal region Cys mutants. Immunoblot analysis was performed as described in the legend of Figure 3 using anti-polyhistidine (A) and anti-AcrB (B) antibodies.

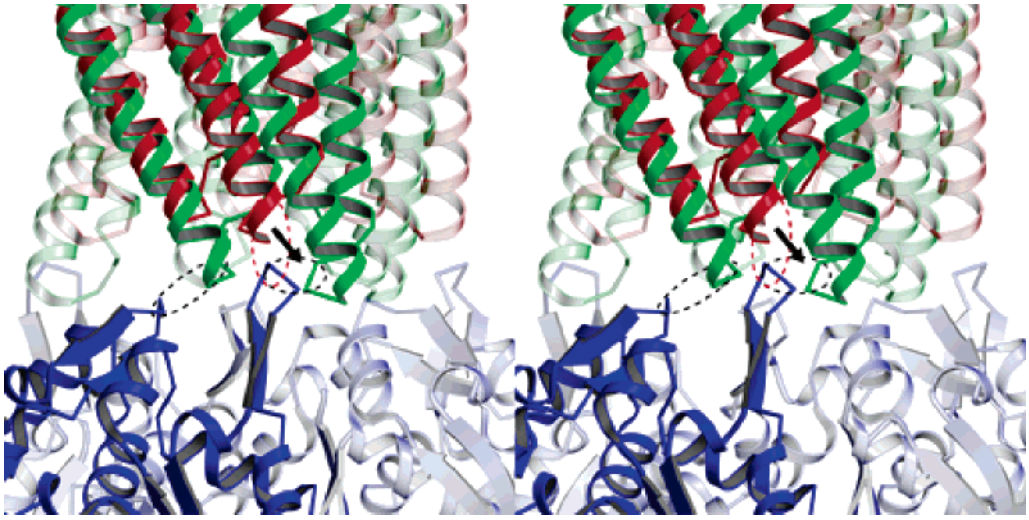

FIGURE 6: Putative two-step model of the AcrB−TolC interaction. AcrB (blue) comes into tip-to-tip contact with TolC (red) and then docks tightly with TolC (green). The local conformations around the docking sites of AcrB and TolC at the stable contact stage might be changed from the model shown in Figure 2.

(*9*). In addition, the slightly tilted structure of the C-terminal vertical hairpin may correspond to the twisted-up structure of the TolC coiled coil, and when in the contact state, the C-terminal hairpin may be standing up straight like the N-terminal one. Thus, at the first tip-to-tip contact stage, the C-terminal regions might not be in contact. That is the reason the degree of cross-linking in the C-terminal region is lower than that in the N-terminal region. The only contact site in TolC is position 365, which appears to be next to the tip in the close-up view (Figure 2B). On the other hand, positions 795 and 796 in AcrB are at the tip of the hairpin. Therefore, a conformational change should occur to close these positions in the deep contact stage.

TolC is a multifunctional outer membrane channel that couples with a wide variety of inner membrane transporters besides AcrAB (*25*). However, the amount of TolC in the outer membrane is not enough to form permanent complexes with all of these inner membrane transporters. Therefore, we proposed a transient complex model in which substrate binding to AcrB triggers formation of the AcrAB−TolC complex (*26*). If this is so, complex formation should depend on the presence of a substrate. Surprisingly, disulfide

complex formation in this experiment was not affected by the addition of acriflavine, suggesting alternative possibilities. (i) The transient complex formation by AcrB and TolC itself is independent of the substrate, or (ii) an unknown intrinsic substrate exists in the cytoplasm, which facilitates complex formation. The latter possibility is also supported by the fact that the *acrAB* gene is almost constitutively expressed despite the presence of the repressor AcrR (*27*).

Complex formation may also be independent of proton motive force energy coupling, because the complex was observed in putative proton translocation-deficient mutant D407A. This observation is consistent with the finding of Thanabalu et al. that the assembly of the HlyBD−TolC complex does not need ATP hydrolysis (*28*). Energy might be required when AcrB pumps out substrates into a TolC channel after complex formation.

Tikhonova and Zgurskaya reported that the AcrAB−TolC complex was detected in sucrose gradient fractionation and copurification studies (*17*). They showed that, in the absence of AcrA, the amount of AcrB detected in the outer membrane fraction was far smaller than that in the presence of AcrA, indicating the important role of AcrA in ternary complex formation. On the contrary, disulfide complex formation was not affected by the deletion of AcrA in our experiment. Our observation could be explained in terms of the fact that the transient complex formation itself is independent of AcrA, while the complex may be fixed with AcrA. Since disulfide bonding, having once occurred, is stable, disulfide complex formation might be independent of AcrA.

AcrA has a signal sequence at its N-terminus, which is cleaved and then modified by a lipid moiety. This modification is not essential for the export of substrates in vitro (*29*). AcrA interacts physically with AcrB, as revealed in coimmunoprecipitation (*16*) and chemical cross-linking experiments (*15*). The MexAB−OprM (AcrAB−TolC homologues) complex has also been detected via copurification (*30*). Recently, the crystal structure of MexA was determined at 2.4 Å (*13*). The predicted MexAB−OprM complex model proposes that MexB docks directly with OprM, and MexA is on the periplasmic side of the MexB−OprM complex. In addition, a conformational change and oligomerization of AcrA are induced by a pH change (*31*). The interaction between AcrA and TolC has also been detected physiologically (*18*). Furthermore, Fernamdez-Recio et al. suggested that AcrB docks directly with TolC in the tripartite complex model (*32*). These previously reported observations are all consistent with our current proposed hypothesis that AcrB (or MexB) first directly interacts with TolC (or OprM) and then the complex is stabilized by AcrA (or MexA).

REFERENCES

1. Nishino, K., and Yamaguchi, A. (2001) Analysis of a complete library of putative drug transporter genes in *Escherichia coli*, *J. Bacteriol. 183*, 5803−5812.
2. Sulavik, M. C., Houseweart, C., Cramer, C., Jiwani, N., Murgolo, N., Greene, J., DiDomenico, B., Shaw, K. J., Miller, G. H., Hare, R., and Shimer, G. (2001) Antibiotic susceptibility profiles of *Escherichia coli* strains lacking multidrug efflux pump genes, *Antimicrob. Agents Chemother. 45*, 1126−1136.
3. Murakami, S., Nakashima, R., Yamashita, E., and Yamaguchi, A. (2002) Crystal structure of bacterial multidrug efflux transporter AcrB, *Nature 419*, 587−593.
4. Nikaido, H., Basina, M., Nguyen, V., and Rosenberg, E. Y. (1998) Multidrug efflux pump AcrAB of *Salmonella typhimurium* excretes only those β-lactam antibiotics containing lipophilic side chains, *J. Bacteriol. 180*, 4686−4692.
5. Dinh, T., Paulsen, I. T., and Saier, M. H. (1994) A family of extracytoplasmic proteins that allow transport of large molecules across the outer membranes of Gram-negative bacteria, *J. Bacteriol. 176*, 3825−3831.
6. Tseng, T. T., Gratwick, K. S., Kollman, J., Park, D., Nies, D. H., Goffeau, A., and Saier, M. H. (1999) The RND permease superfamily: An ancient, ubiquitous and diverse family that includes human disease and development proteins, *J. Mol. Microbiol. Biotechnol. 1*, 107−125.
7. Paulsen, I. T., Park, J. H., Choi, P. S., and Saier, M. H. (1997) A family of Gram-negative bacterial outer membrane factors that function in the export of proteins, carbohydrates, drugs and heavy metals from Gram-negative bacteria, *FEMS Microbiol. Lett. 156*, 1−8.
8. Fralick, J. A. (1996) Evidence that TolC is required for functioning of the Mar/AcrAB efflux pump of *Escherichia coli*, *J. Bacteriol. 178*, 5803−5805.
9. Koronakis, V., Sharff, A., Koronakis, E., Luisi, B., and Hughes, C. (2000) Crystal structure of the bacterial membrane protein, TolC, central to multidrug efflux and protein export, *Nature 405*, 914−919.
10. Eswaran, J., Hughes, C., and Koronakis, V. (2003) Locking TolC entrance helices to prevent protein translocation by the bacterial type I export apparatus, *J. Mol. Biol. 327*, 309−315.
11. Matias, V. R., Al-Amoudi, A., Dubochet, J., and Beveridge, T. J. (2003) Cryo-transmission electron microscopy of frozen-hydrated sections of *Escherichia coli* and *Pseudomonas aeruginosa*, *J. Bacteriol. 185*, 6112−6118.
12. Murakami, S., Tamura, N., Saito, A., Hirata, T., and Yamaguchi, A. (2004) Extramembrane central pore of multidrug exporter AcrB in *Escherichia coli* plays an important role in drug transport, *J. Biol. Chem. 279*, 3743−3748.
13. Akama, H., Matsuura, T., Kashiwagi, S., Yoneyama, H., Narita, S., Tsukihara, T., Nakagawa, A., and Nakae, T. (2004) Crystal structure of the membrane fusion protein, MexA, of the multidrug transporter in *Pseudomonas aeruginosa*, *J. Biol. Chem. 279*, 25939−25942.
14. Higgins, M. K., Bokma, E., Koronakis, E., Hughes, C., and Koronakis, V. (2004) Structure of the periplasmic component of a bacterial drug efflux pump, *Proc. Natl. Acad. Sci. U.S.A. 101*, 9994−9999.
15. Zgurskaya, H. I., and Nikaido, H. (2000) Cross-linked complex between oligomeric periplasmic lipoprotein AcrA and the inner-membrane-associated multidrug efflux pump AcrB from *Escherichia coli*, *J. Bacteriol. 182*, 4264−4267.
16. Kawabe, T., Fujihira, E., and Yamaguchi, A. (2000) Molecular construction of a multidrug exporter system, AcrAB: Molecular interaction between AcrA and AcrB, and cleavage of the N-terminal signal sequence of AcrA, *J. Biochem. 128*, 195−200.
17. Tikhonova, E. B., and Zgurskaya, H. I. (2004) AcrA, AcrB, and TolC of *Escherichia coli* form a stable intermembrane multidrug efflux complex, *J. Biol. Chem. 279*, 32116−32124.
18. Touzé, T., Eswaran, J., Bokma, E., Koronakis, E., Hughes, C., and Koronakis, V. (2004) Interactions underlying assembly of the *Escherichia coli* AcrAB-TolC multidrug efflux system, *Mol. Microbiol. 53*, 697−706.
19. Yanisch-Perron, C., Vieira, J., and Messing, J. (1985) Improved M13 phage cloning vectors and host strains: Nucleotide sequences of the M13mp18 and pUC19 vectors, *Gene 33*, 103−119.
20. Kunkel, T. A. (1985) Rapid and efficient site-specific mutagenesis without phenotypic selection, *Proc. Natl. Acad. Sci. U.S.A. 82*, 488−492.
21. Yamamoto, T., and Yokota, T. (1981) *Escherichia coli* heat-labile enterotoxin genes are flanked by repeated deoxyribonucleic acid sequences, *J. Bacteriol. 145*, 850−860.
22. Kobayashi, N., Nishino, K., and Yamaguchi, A. (2001) Novel macrolide-specific ABC-type efflux transporter in *Escherichia coli*, *J. Bacteriol. 183*, 5639−5644.
23. Link, A. J., Phillips, D., and Church, G. M. (1997) Methods for generating precise deletions and insertions in the genome of wild-type *Escherichia coli*: Application to open reading frame characterization, *J. Bacteriol. 179*, 6228−6237.
24. Laemmli, U. K. (1970) Cleavage of structural proteins during the assembly of the head of bacteriophage T4, *Nature 227*, 680−685.

25. Koronakis, V., Eswaran, J., and Hughes, C. (2004) Structure and function of TolC: The bacterial exit duct for proteins and drugs, *Annu. Rev. Biochem. 73*, 467−489.
26. Murakami, S., and Yamaguchi, A. (2003) Multidrug-exporting secondary transporters, *Curr. Opin. Struct. Biol. 13*, 443−452.
27. Ma, D., Alberti, M., Lynch, C., Nikaido, H., and Hearst, J. E. (1996) The local repressor AcrR plays a modulating role in the regulation of *acrAB* genes of *Escherichia coli* by global stress signals, *Mol. Microbiol. 19*, 101−112.
28. Thanabalu, T., Koronakis, E., Hughes, C., and Koronakis, V. (1998) Substrate-induced assembly of a contiguous channel for protein export from *E. coli*: Reversible bridging of an inner-membrane translocase to an outer membrane exit pore, *EMBO J. 17*, 6487−6496.
29. Zgurskaya, H. I., and Nikaido, H. (1999) Bypassing the periplasm: Reconstitution of the AcrAB multidrug efflux pump of *Escherichia coli*, *Proc. Natl. Acad. Sci. U.S.A. 96*, 7190−7195.
30. Mokhonov, V. V., Mokhonova, E. I., Akama, H., and Nakae, T. (2004) Role of the membrane fusion protein in the assembly of resistance-nodulation-cell division multidrug efflux pump in *Pseudomonas aeruginosa*, *Biochem. Biophys. Res. Commun. 322*, 483−489.
31. Ip, H., Stratton, K., Zgurskaya, H., and Liu, J. (2003) pH-induced conformational changes of AcrA, the membrane fusion protein of *Escherichia coli* multidrug efflux system, *J. Biol. Chem. 278*, 50474−50482.
32. Fernandez-Recio, J., Walas, F., Federici, L., Venkatesh Pratap, J., Bavro, V. N., Miguel, R. N., Mizuguchi, K., and Luisi, B. (2004) A model of a transmembrane drug-efflux pump from Gram-negative bacteria, *FEBS Lett. 578*, 5−9.
33. Lawrence, M. C., and Colman, P. M. (1993) Shape complementarity at protein/protein interfaces, *J. Mol. Biol. 234*, 946−950.
34. Richards, F. M. (1977) Areas, volumes, packing and protein structure, *Annu. Rev. Biophys. Bioeng. 6*, 151−176.
35. Kraulis, P. J. (1991) MOLSCRIPT: A program to produce both detailed and schematic plots of protein structures, *J. Appl. Crystallogr. 24*, 946−950.
36. Merritt, E. A., and Bacon, D. J. (1997) Raster3D photorealistic molecular graphics, *Methods Enzymol. 277*, 505−524.

BI050452U